COBEM 2023 27TH INTERNATIONAL CONGRESS OF MECHANICAL ENGENEERING

ABCM Brazilian Society of Mechanical Sciences and Engineering
27th ABCM International Congress of Mechanical Engineering
December 04-08, 2023, Florianópolis-SC, Brazil

COB-2023-1603
MODELING THE DYNAMIC OPERATION OF A MAGNETIC REFRIGERATOR VIA RECURRENT NEURAL NETWORKS

Pedro Miola Silva[a]
pedro.silva@polo.ufsc.br
Yan Azeredo[a]
yan.azeredo@polo.ufsc.br
Anderson Martins Lorenzoni[a]
anderson.lorenzoni@polo.ufsc.br
Guilherme Fidelis Peixer[a]
guilherme.peixer@polo.ufsc.br
Rodolfo César Costa Flesch[b]
rodolfo.flesch@ufsc.br
Jaime Andrés Lozano Cadena[a]
jaime@polo.ufsc.br
Jader Riso Barbosa Jr.[a]
jrb@polo.ufsc.br

[a] POLO – Research Laboratories for Emerging Technologies in Cooling and Thermophysics, Department of Mechanical Engineering, Federal University of Santa Catarina, Florianópolis, SC, 88040-900, Brazil

[b] LabMetro – Metrology and Automation Laboratory, Department of Mechanical Engineering, Federal University of Santa Catarina, Florianópolis, SC, 88040-900, Brazil

Abstract. *Environmental concerns and governmental policies have recently increased pressure on the refrigeration industry. Various technologies have been explored to overcome this problem, and magnetocaloric refrigeration systems are one of the most promising long-term alternatives. Despite recent prototype developments, this technology is still not competitive enough with vapor compression systems, especially because of high energy consumption. To improve this issue, dynamic models can provide valuable insights into the transient operation of the system. This work is focused on the development of a Neural Network aiming to model the dynamic operation of a large-scale magnetic refrigeration system, designed for air-conditioning applications. Through a Design of Experiments methodology, the excitation signals for the identification experiment were proposed, with five actuation signals and three disturbances selected to compose the models, and the output temperature of the cold manifold as the target parameter. A nonlinear autoregressive neural network with exogenous inputs was selected to model the transient operation of the system, and a three-step hyperparameter optimization was performed. The temperature model achieved an R^2 of 0.942 with a 0.27°C mean residual for 1-step-ahead prediction and an R^2 of 0.852 with a 0.42°C mean residual for 90-step-ahead predictions.*

Keywords: *magnetocaloric refrigeration, artificial intelligence, machine learning, recurrent neural networks, active magnetic regenerator*

1. INTRODUCTION

Refrigeration is a technology that plays a crucial role in the development of modern society. From allowing food conservation for extended periods of time and providing thermal comfort in different regions of the planet to enabling the thermal management and temperature control of components and processes, it is a technology usually taken for granted by the general population given its impact and importance. The most common refrigeration technology is based on the mechanical compression and expansion of a refrigerant fluid. After being the standard technology and optimized for more than a century, these systems are mature in terms of efficiency and cost. Despite that, the use of volatile refrigerants has become a major concern in recent decades as a result of their environmental impact and the toxicity and flammability aspects. According to the 2019 International Institute of Refrigeration Report (IIR, 2019), 7.8% of the global greenhouse effect gas emissions are related to the refrigeration sector, of which HFC$_S$ and HCFC$_S$ represent 37%. Furthermore, 17% of the total electric energy is consumed by heating and cooling systems, while demand for the latter is expected to triple by 2050. This stimulates both industry and academia to develop more efficient systems that operate with a smaller carbon footprint.

One of the most promising alternatives to overcome this issue is magnetocaloric cooling, which has a perspective for commercial applications in the long run (Qian *et al.*, 2016). The technology is based on the Magnetocaloric Effect (MCE), which is the thermal response of certain materials when a magnetic field is applied to them. In addition to the reversible behavior of the MCE in many Magnetocaloric Materials (MCM), which makes them ideal for high-efficiency systems, the refrigerant is employed in the solid phase, so leakage is not a concern. However, the low magnitude of MCE is a major drawback, which has led to the use of the active magnetic regenerator (AMR) cycle in most modern magnetocaloric refrigeration prototypes. In this configuration, MCMs are employed as porous matrices that serve as solid refrigerants and regenerative matrices, providing temperature ranges that are appropriate for refrigeration applications.

In recent years, Magnetic Refrigeration (MR) technologies for room-temperature operation have been advanced with the development of different prototypes, such as the heat pump developed by Dall'Olio *et al.* (2021), the wine cooler developed by Nakashima *et al.* (2021), and the air conditioner developed by Peixer *et al.* (2023b). Although these developments show an increasing maturity in MR research, they are not competitive with vapor compression technologies in terms of cooling capacity and coefficient of performance (COP). In the work of Peixer *et al.* (2023b), an air conditioner operated by a magnetic refrigeration system was developed to achieve a cooling capacity of 9000 BTU/h (2637 W) with ambient temperature hot and cold of 35 °C and 22 °C, respectively. However, preliminary results show that the power supplied to the prototype remains a barrier to competitiveness with established technologies. One of the main challenges of these systems is the complexity required in the modeling process, which involves heat transfer, thermodynamics, fluid mechanics, and magnetostatic domains and has been mainly tackled by numerical approaches (Vieira *et al.*, 2020). However, given the computational cost involved, transient modeling has not been explored in a deep way in the literature (Nakashima *et al.*, 2022), although it is of great importance for the energy consumption of refrigeration systems (Hermes and Melo, 2008).

For that, this work seeks to develop a transient model for the operation of the prototype developed by Peixer *et al.* (2023b). Aiming for the high accuracy and low computational cost involved, a machine learning-based methodology was selected as the modeling tool, more specifically by training a recurrent neural networks on a dataset, specifically designed for the development of a transient model of the system.

2. METHODOLOGY

To start the modeling of the apparatus, an identification test was performed in an air conditioner operated by a magnetic refrigeration system developed by Peixer *et al.* (2023b), to collect a data set representative of the dynamic operation of the prototype. For that, initially a brief discussion of the experimental apparatus of the Magnetic Refrigeration Unit (MRU) is made, covering its main subsystems and the calorimeter used to perform the tests. The design of the methodology of the experiments performed for the identification of the prototype is then presented, detailing how the amplitude and frequencies of the signals were determined. Lastly, the model design is approached, discussing the Neural Network architecture, its parameters, optimization, and validation methodology.

2.1 Experimental Apparatus

The prototype of the present study consists of a large-scale magnetic refrigeration system. The device was designed to achieve a cooling capacity of 9000 BTU/h, operating between reservoir temperatures of 22°C and 35°C (Peixer *et al.*, 2023a). The system is composed of four main subsystems, namely: the AMR, the magnetic circuit (MC), the hydraulic and controls system (HCS), and the heat exchangers (HEx). The performance evaluation and experimental tests of the prototype were carried out in a calibrated calorimeter, designed and commissioned specifically for the experimentation of the MRU.

2.1.1 Magnetic Circuit

The MC is the component responsible for providing the magnetic flux density for the MCM. It is composed of two concentric cylinders, arranged in a configuration known as rotor-stator. The outer cylinder, also known as the rotor, consists of hard and soft ferromagnetic materials. The hard ones are composed of 64 epoxy-glued segments of Nd-Fe-B permanent magnets of grades N50M and N42M, with remanence directions designed to optimize the magnetic flux density in the gap between the rotor and the stator (Fortkamp *et al.*, 2023). The total volume of permanent magnets is 12.5 L. The soft ferromagnetic region is made up of S235JR laminated sheets, solemnly for manufacturing purposes. A servomotor (WEG-SWA-56-4-8-20, driver WEG-SCA06) coupled to a pulley and belt arrangement is responsible for the rotation of the rotor. On the other hand, the inner cylinder, also known as the stator, remains static and is responsible for positioning the AMRs and guiding the magnetic flux density. The stator is made up of 0.5 mm hollow circular laminated sheets of E-145 electrical steel, to reduce eddy currents. The sheets are stacked around a fixed shaft and tied by two flanges. A cross-sectional view of a schematic representation of the MC-AMR assembly, where the rotor, stator, shaft, and AMR can be observed, is presented in Fig. 1.

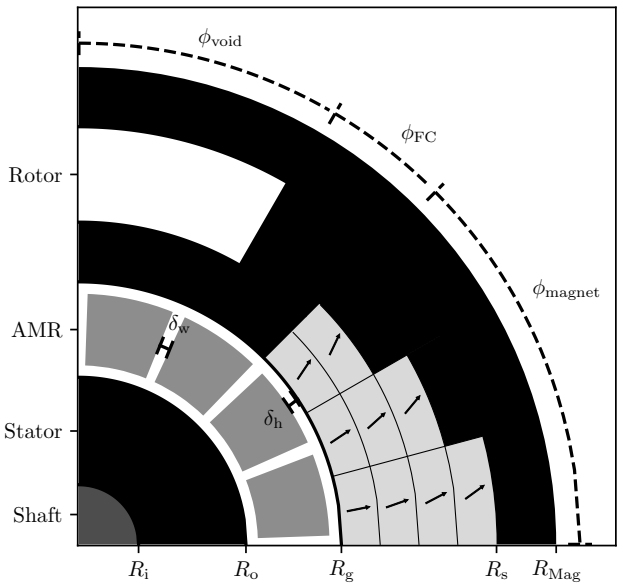

Figure 1. Cross section view of the MC-AMR assembly. Black regions: soft magnetic material; white regions: air; light gray regions: hard magnetic material; gray regions: AMRs; Dark gray region at the bottom left: stator/shaft; arrows: remanence directions Peixer *et al.* (2023a).

The dimensions of R_{Mag}, R_{s}, R_{g}, R_{o} and R_{i} are, respectively, 338, 315, 185, 153, and 34 mm. The length of both the rotor and the stator is 190 mm. The dimensions of δ_{h} is 2 mm and that of δ_{w} is 2.5 mm.

2.1.2 Active Magnetic Regenerator

The AMRs consist of stainless steel casings attached to the stator with porous beds of MCM housed inside and remain static during operation. The casings have a cylindrical shell shape and were designed to withstand cyclical mechanical loads with a minimum thickness (Peixer *et al.*, 2017). The porous medium is made up of 11 layers of which 10 are La(FeMnSi)$_{13}$H$_z$ alloys (commercialized as *Calorivac-HS2* by Vacuumschmelze GmbH & Co) with an elongated cylinder shape and different Curie Temperature, T_{Curie} and one is Gd (supplied by the Baotou Research Institute of Rare Earths, China) with a spherical shape (Vieira *et al.*, 2020). This layout is utilized to overcome the reduction in the MCE typical of first order MCM, ensuring that every layer is close to its T_{Curie}, where the peak of the effect occurs (Peixer *et al.*, 2023a). The number of layers and their T_{Curie} were established according to the availability of materials and the requirements of the system temperature. The porous bed has a length of 129 mm and the internal cross section of the casing has a mean height and width of 24.8 mm and 52 mm, respectively. The optimal AMR configuration in terms of Curie temperature and mass fraction was determined by numerical solution by Vieira *et al.* (2020) as shown in the Tab. 2.1.2 There are 16 AMR beds assembled in the stator and their Gd and La(FeMnSi)$_{13}$H$_z$, each one is composed on average of 254 g of Gd and 486 g of La(FeMnSi)$_{13}$H$_z$, with an average porosity of 44%.

Table 1. Curie temperatures of each layer of the AMRs.

Layer	**Material**	**T$_{Curie}$ [ºC]**	**Mass fraction [%]**
1	La(Fe,Mn,Si)$_{13}$H$_y$	15.0	7.6
2	La(Fe,Mn,Si)$_{13}$H$_y$	16.8	7.6
3	Gd	17.0	24.0
4	La(Fe,Mn,Si)$_{13}$H$_y$	19.3	7.6
5	La(Fe,Mn,Si)$_{13}$H$_y$	22.2	7.6
6	La(Fe,Mn,Si)$_{13}$H$_y$	24.6	7.6
7	La(Fe,Mn,Si)$_{13}$H$_y$	27.9	7.6
8	La(Fe,Mn,Si)$_{13}$H$_y$	30.0	7.6
9	La(Fe,Mn,Si)$_{13}$H$_y$	32.6	7.6
10	La(Fe,Mn,Si)$_{13}$H$_y$	34.6	7.6
11	La(Fe,Mn,Si)$_{13}$H$_y$	36.4	7.6

2.1.3 Hydraulic and Controls System

The hydraulic and control system is responsible for managing the fluid flow and making sure that each component has the appropriate mass flow rate and frequency. The fluid consists of a mixture of water (95%) and anticorrosive fluid (5%). An arrangement of gear pump (Thebe P11/7 5 hp), solenoid valves (ASCO SC8210-112) and check valves (Puma AE-10) is employed according to the hydraulic diagram presented in Fig. 2 to guarantee the oscillatory flow in the AMRs and continuous flow in the remaining components (Santos *et al.*, 2021). Each pair of AMRs is controlled by a pair of solenoid valves and two pairs of check valves. Valve actuation is controlled by the signal of an encoder coupled to the rotor. Hall-effect sensors are used to monitor the coupling between the hydraulic and magnetic profiles.

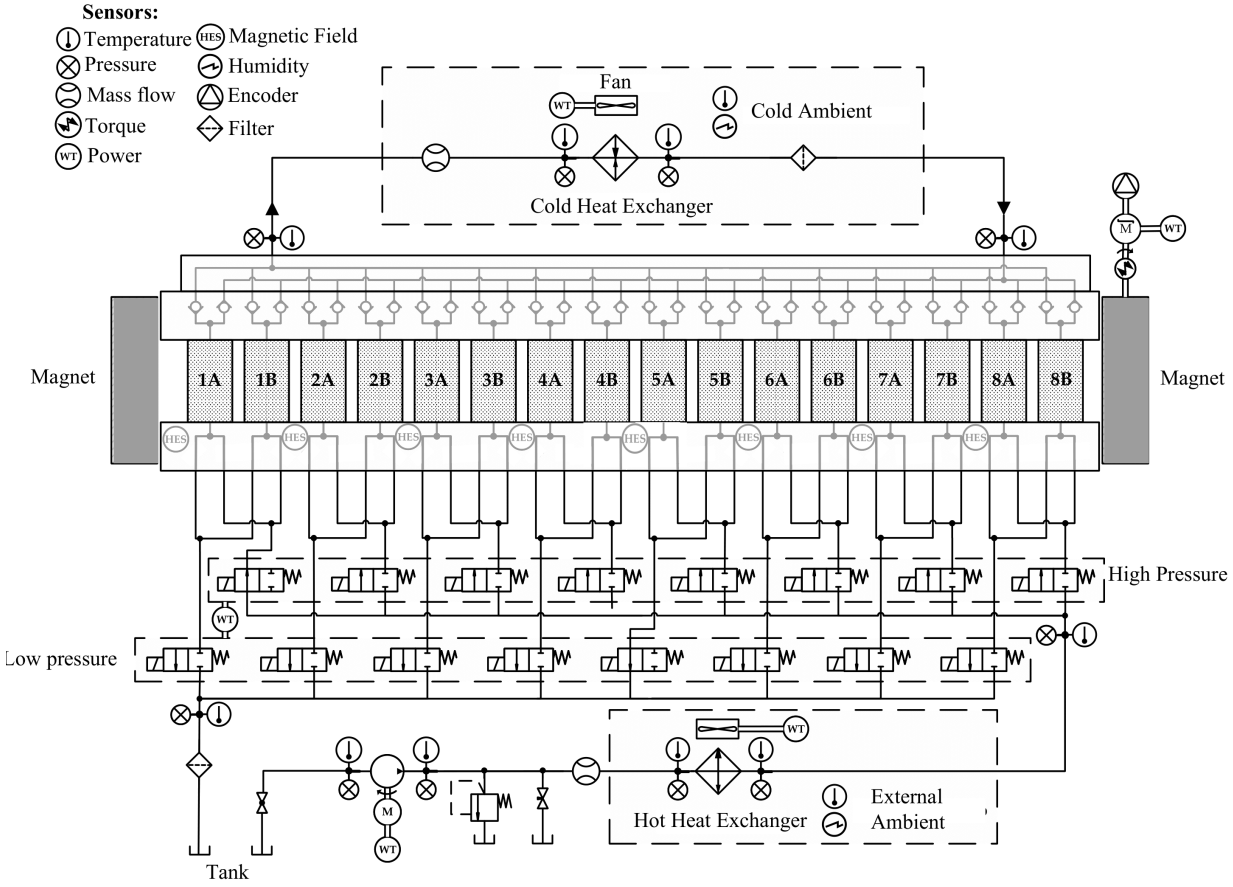

Figure 2. Hydraulic Diagram of the MRU.

Temperature and pressure are acquired at different positions in the fluid line and in the ambient environment. Power transducers are used in fans, pump, and rotor, which also has a torque meter. The measurement of mass flow is performed before the CHEx and HHEx. The angular position of the rotor and the magnetic flux are acquired by an encoder and 8 Hall-Effect sensors, respectively. Data acquisition and control are performed with LabVIEW software with National Instruments hardware (cDAQ-9179 and My-Rio 19000).

2.1.4 Heat Exchangers and Calorimeter

The HEx are responsible for providing the thermal contact between the working fluid and the hot and cold heat reservoirs. For their favorable thermal-hydraulic characteristics, fan-supplied multicircuited herringbone-wave tube fin HExs were used (Peixer *et al.*, 2022). The HExs employed in the MRU have 515 mm height, 550 mm width and 245 mm length, with eight fins-per-inch, a tube internal diameter of 11.9 mm and wall thickness of 0.4 mm. To force convection, each HEx has an axial fan (Ebm-Papst S4E350-AN19-43).

The calorimeter consists of two chambers separated by an insulated wall that reproduces the outdoor (hot) and indoor (cold) ambients. The MRU is positioned in the former, whereas the CHEx is positioned in the latter. The walls are insulated with polyisocyanurate which has a thermal conductivity between 0.02 and 0.03 $\mathrm{Wm^{-1}K^{-1}}$. The internal wall

separating the chambers has a thickness of 150 mm, while the other ones have 70 mm. Pressure, temperature, humidity, power consumption, and condensed water mass are measured in calorimeter.

A picture of the MRU outside the calorimeter is presented in Fig. 3. An explanatory video of the MRU and the calorimeter can be found in: https://youtu.be/5lVMstvAjgk. A complete description of the MRU can be found in Peixer *et al.* (2023b) and the calorimeter in Silva *et al.* (2021).

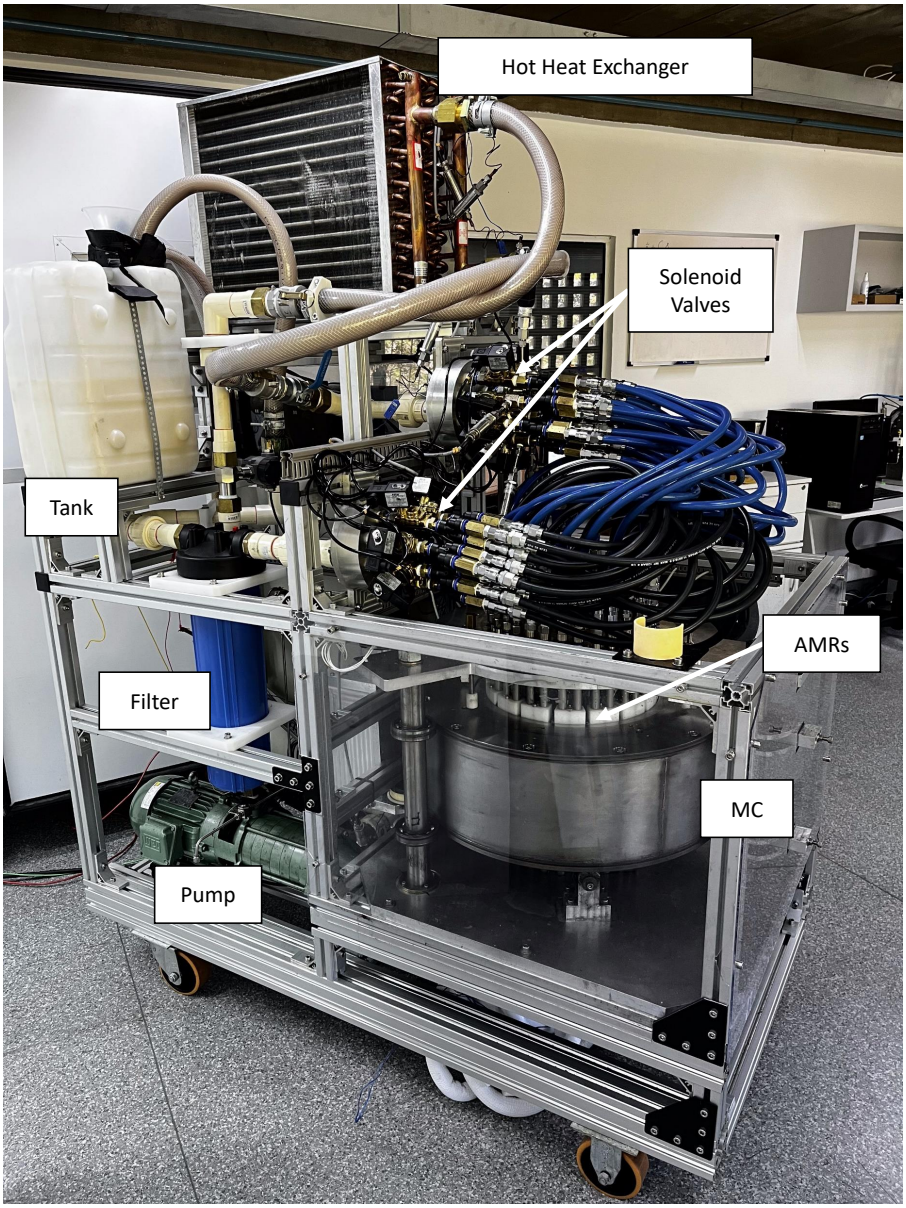

Figure 3. Magnetic Refrigeration Unit

2.2 Design of Experiments

The design of the experiments was carried out according to the methodology proposed by Doyle *et al.* (2002). The first step consists of the determination of the parameters that make up the output target and the input space. The temperature of the hot blow in the AMR outlet ($T_{\mathrm{HB,out}}$) is chosen as the output of the process for the model. This is due to the variable being the lowest temperature of the system, its use in magnetic refrigerators as a benchmark between different prototypes and, lastly, the fact that it has a faster response than the cold ambient temperature $T_{\mathrm{amb,cold}}$. Furthermore, five actuation signals were selected, namely: AMR magnetization frequency (f_{AMR}), power supplied to the pump ($\dot{W}_{\mathrm{pump}}$), blow fraction ($B_{\%}$), power supplied to the hot side fan ($\dot{W}_{\mathrm{fan,hot}}$) and power supplied to the cold side fan ($\dot{W}_{\mathrm{fan,cold}}$). Furthermore, the cold and hot ambient temperatures ($T_{\mathrm{amb,hot}}$, $T_{\mathrm{amb,cold}}$) and the temperature of the cold blow at the AMR outlet ($T_{\mathrm{CB,out}}$) are also included as disturbances and measured during experiments due to their influence on the results.

To design the excitation signals, the amplitude of each of the input variables was analyzed. The minimum value of f_{AMR} was set at 0.1 Hz, to prevent loss in system cooling capacity, while the maximum was set at 1 Hz, to avoid instabilities in solenoid valve operation. The minimum value of $B_{\%}$ was set as 20%, also to avoid loss in system cooling capacity, while the maximum value was set as 40%, to prevent recirculation among AMRs. Regarding $\dot{W}_{\mathrm{pump}}$, the minimum value was set as 30% of the nominal power, when the flow rate becomes too low to allow proper operation of the system, while the maximum value was set at 73%, to avoid system operation at pressures higher than 8 bar. Lastly, for $\dot{W}_{\mathrm{fan,hot}}$ and $\dot{W}_{\mathrm{fan,cold}}$, the minimum and maximum values of the actuation signals were set at 0% and 100% of the nominal power, respectively, since there are no direct restrictions on the operation of the fan.

For the determination of the excitation hold time, the time constant, *i.e.*, the time it takes for $T_{\mathrm{HB,out}}$ to reach 63.2% of its steady state value was measured at an operation with f_{AMR} of 0.5 Hz, $\dot{W}_{\mathrm{pump}}$ of 44% , $B_{\%}$ of 35%, $\dot{W}_{\mathrm{fan,hot}}$ of 100% and $\dot{W}_{\mathrm{fan,cold}}$ of 100%, considered as a point at which the system is expected to operate. The value encountered for the time constant, τ, was 600 s. Therefore, each hold time of the test was defined between τ and 1.5τ, chosen by a random algorithm. The number of points in the test was defined as 80, which ensured that the test would not exceed a total duration of 20 hours.

Next, it is necessary to determine the distribution of the test points. Different methodologies are available for that, such as random, D-optimal, and Latin Hypercube (Deflorian and Zaglauer, 2011). In the present work, the Latin Hypercube strategy was employed. With that, the last step of the identification process consists in designing the shape of the sequence. For the present case, an adapted version of the Amplitude Modulated Pseudo-Random Binary Signal was employed, where the different amplitudes of the signal are excited only in one frequency, given the knowledge that low frequencies dominate the behavior of the thermal process under evaluation. Three different data sets were created according to the methodology described above: a training set, used for the training of the models, a validation set, used for the optimization of the hyperparamereters of the model, and a test set, used for the evaluation of the generalization of the model.

2.3 Model Design

The model selected for the identification of the system was a nonlinear autoregressive model with exogenous inputs (NARX). It was selected given the previous knowledge of the capability of Neural Networks in magnetic refrigeration systems (Peixer *et al.*, 2023a). The NARX structure shown in Figure 4 is composed of time delay lines, with size m for inputs and n for outputs, that allow the network to use past values from inputs $u(t-m)$ and outputs $y(t-n)$ to make prediction $\hat{y}$, a recurrency to return predicted outputs, and a multilayer perceptron neural network (MLP). A MLP consists of a ANN with high connectivity, neurons with nonlinear activation functions, and layers hidden from the input and output nodes (Haykin, 2009). The implementation of ANNs was done in Python with the SysIdentPy library (Lacerda Jr. *et al.*, 2020).

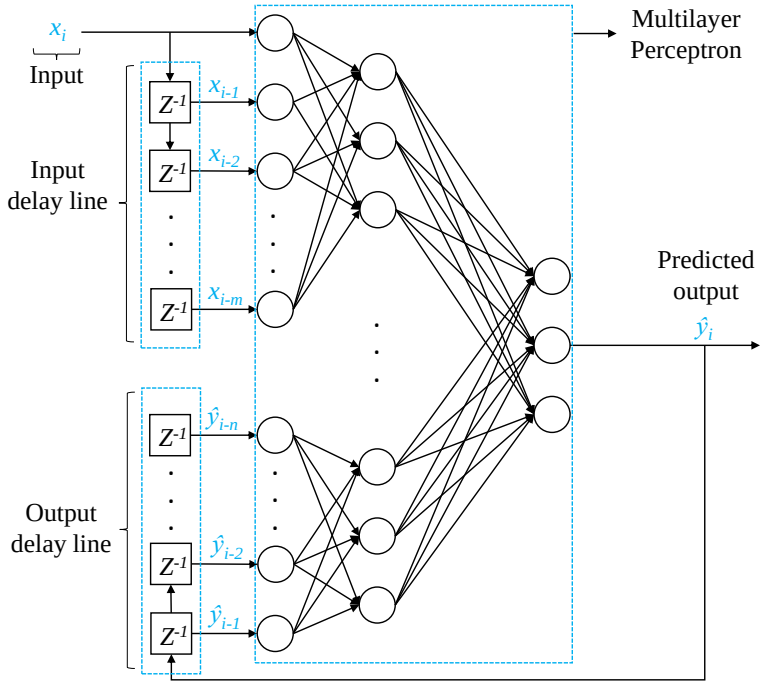

Figure 4. NARX neural network structure. Adapted from Haykin (2009)

The hyperparameter optimization of the neural network consisted of three steps for random searches. In the first one,

the effect of the hyperparameters depicted in Tab. 2 was evaluated by the training results of 2000 models. From them, the 50 best models were selected based on the resulting coefficient of determination in the validation set, which went through the second hyperparameter optimization round, this time only via the learning rate. Lastly, the best model went through the last hyperparameter optimization round, where its learning rate was again optimized.

Table 2. Search space for the random search.

Feature	**Search space**
Learning rate	$1e-4$, $2.5e-4$, $5e-4$, $7.5e-4$, $1e-3$, $2.5e-3$, $e5e-3$, $7.5e-3$ or $1e-2$
Neurons	5, 10, 15, 20, 25, 30, 35 or 40
Hidden layers	2, 3, 4 or 5
Input lags	1 to 5
Output lags	1 to 5

The training of the Neural Network was carried out with the Adam as optimizer. A hyperbolic tangent was employed as an activation function in the hidden layers. The batch size and the number of training epochs were fized at 1000 and 100, for all of the hyperparameter steps. The loss function employed was the mean squared error.

3. RESULTS

The resulting values for the hyperparameters of the NARX network after the three-step optimization carried out in this work are shown in Tab. 3.

Table 3. Hyperparameters of the final NARX configuration.

Feature	**Parameter**
Learning rate	$8.25e-3$
Hidden layers	5
Neurons per layer	1^{st}: 30, 2^{nd}: 5, 3^{rd}: 30, 4^{th}: 10, 5^{th}: 30
Input lags	4
Output lags	1

The prediction of temperature of the selected model for 1-step-ahead and its prediction residual, both in °C and in perceptual values, are displayed in Fig;5.

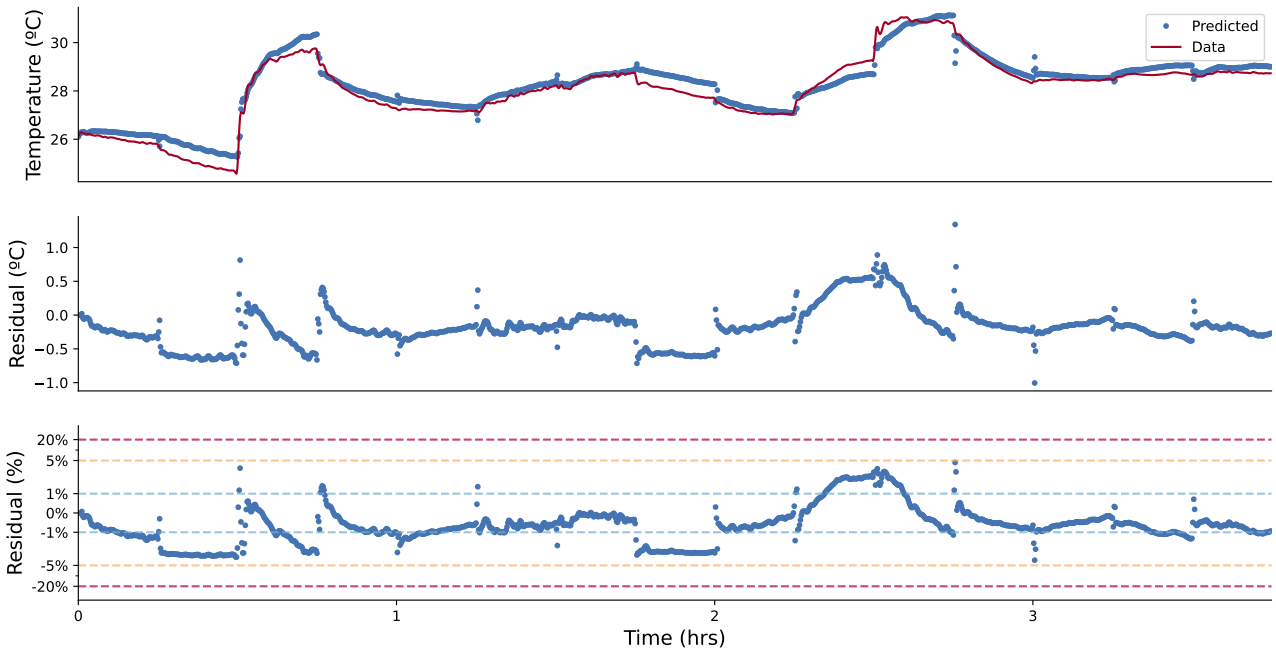

Figure 5. Temperature prediction of the selected model for 1 step ahead and its prediction residual.

From the results depicted in Fig. 5 it can be observed that the trained model was able to capture the complex nonlinear phenomena involved in the transient operation of magnetic refrigeration systems. Although there are operating conditions

in which the models fit the results better than the others, in general the results are within a $\pm$ 0.5°C deviation from the original data, with a mean value of 0.27°C. Furthermore, the achieved coefficient of determination for a 1-step advance was 0.942.

Furthermore, the coefficient of determination achieved for the 90-step predictions was 0.852 and the mean temperature deviation was 0.42ºC, both slightly higher than those for the 1-step prediction. This is expected behavior as the deviation from the actual values and predicted ones accumulates as the prediction horizon increases. For a better evaluation of this effect, the influence of the length of the prediction on the coefficient of determination for the temperature model is shown in Fig. 5.

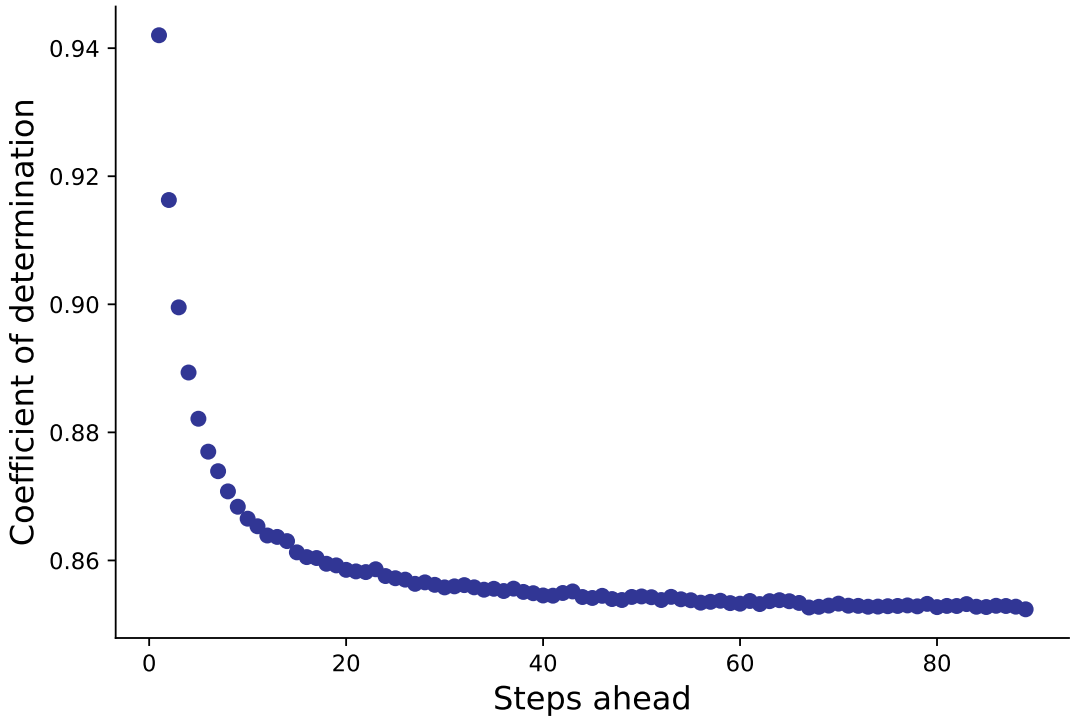

Figure 6. Influence of the prediction length in the coefficient of determination for the temperature model.

The effect of the prediction horizon is clearly visible in Fig. 6. For a 1-step-ahead prediction, the coefficient of determination reaches its maximum value of 0.942 and decreases as one increases the prediction horizon. This is expected since the deviations of the model accumulate at each subsequent prediction point. In the first 20 prediction points there is a sharp drop in the coefficient of determination, and after around 40 steps-ahead a plateau is reached in the values of the coefficient of determination.

To improve the results obtained by the models, different neural network architectures, such as long-short-term memory (Hochreiter and Schmidhuber, 1997) or echo-state neural networks (Schwedersky *et al.*, 2022), can be used, more robust hyperparameter optimization can be performed with methods such as Hyperband (Li *et al.*, 2017) and with strategies such as weight decay or learning rate schedule, or multistep ahead loss functions (Xiong *et al.*, 2013) can be applied.

4. CONCLUSION

In this work, a model was developed to predict the transient behavior of large-scale magnetocaloric refrigeration systems for the operation of air conditioning systems. A NARX neural network architecture was selected, given its high accuracy and computational cost. A design of experiments approach was selected to perform the tests that generated the data of the training, validation, and test sets. Based on the details of the system operation, the input parameters, and their respective design space, the output targets and disturbances were determined.

Three different data sets were generated according to the signals determined with the methodology of the design of the experiments used. The training set was used to train the NARX neural network according to the backpropagation algorithm. The validation set was used to perform a hyperparameter optimization of the learning rate, number of neurons and hidden layers, and input and output lags. Lastly, after training and hyperpameter optimization of the NARX neural network, the test set was used to evaluate the generalization of the trained model.

The model selected from the modeling process for the temperature contained five hidden layers with 30, 5, 30, 10 and 30 neurons, 4 input lags, 1 output lag, and a LR of 8.25e-3, being trained per 100 epochs. It has achieved an R^2 of

0.942 with a 0.27°C mean residual and a R^2 of 0.852 with a 0.42°C mean residual for short and long range predictions respectively. Among the strategies recommended for improving the performance of the model, one can highlight the evaluation of different neural network strategies, performing more robust hyperparameter optimization and employing different loss functions.

5. ACKNOWLEDGMENTS

Financial support from CNPq, FAPESC, CAPES, CODEMGE, and the EMBRAPII Unit Polo/UFSC is duly acknowledged.

6. REFERENCES

Dall'Olio, S., Masche, M., Liang, J., Insinga, A.R., Eriksen, D., Bjork, R., Nielsen, K.K., Barcza, A., Vieyra, H.A., Biek, N.V., Bez, H.N., Engelbrecht, K. and Bahl, C.R.H., 2021. "Novel design of a high efficiency multi-bed active magnetic regenerator heat pump". *International Journal of Refrigeration*. In press.

Deflorian, M. and Zaglauer, S., 2011. "Design of Experiments for nonlinear dynamic system identification". *International Federation of Automatic Control*.

Doyle, F.J., Pearson, R.K. and Ogunnaike, B.A., 2002. *Identification and control using Volterra models*. Springer.

Fortkamp, F.P., Nakashima, A.T., dos Santos, V.M., Lozano, J.A. and Barbosa, J.R., 2023. "Computationally-efficient optimization of the remanence angles of permanent magnet circuits for magnetic refrigeration". *Journal of Magnetism and Magnetic Materials*, Vol. 569, p. 170429. ISSN 0304-8853.

Haykin, S., 2009. *Neural Networks and Learning Machines*. Pearson.

Hermes, C.J. and Melo, C., 2008. "A first-principles simulation model for the start-up and cycling transients of household refrigerators". *International Journal of Refrigeration*, Vol. 31, No. 8, pp. 1341–1357. ISSN 0140-7007.

Hochreiter, S. and Schmidhuber, J., 1997. "Long short-term memory". *Neural Computation*, Vol. 9, No. 8, pp. 1735–1780.

IIR, 2019. "*The impact of the refrigeration sector on climate change*." Technical report, 35th Informatory Note on Refrigeration Technologies. International Institute of Refrigeration. Technical Report. Paris, France.

Lacerda Jr., W.R., da Andrade, L.P.C., Oliveira, S.C.P. and Martins, S.A.M., 2020. "Sysidentpy: A python package for system identification using narmax models". *Journal of Open Source Software*, Vol. 5, No. 54, p. 2384.

Li, L., Jamieson, K., DeSalvo, G., Rostamizadeh, A. and Talwalkar, A., 2017. "Hyperband: A novel bandit-based approach to hyperparameter optimization". *The Journal of Machine Learning Research*, Vol. 18, No. 1, pp. 6765–6816.

Nakashima, A.T., Fortkamp, F.P., de Sá, N.M., dos Santos, V.M., Hoffmann, G., Peixer, G.F., Dutra, S.L., Ribeiro, M.C., Lozano, J.A. and Barbosa, J.R., 2021. "A magnetic wine cooler prototype". *International Journal of Refrigeration*, Vol. 122, pp. 110–121. ISSN 0140-7007.

Nakashima, A., Peixer, G., Lozano, J. and Barbosa, J., 2022. "A lumped-element magnetic refrigerator model". *Applied Thermal Engineering*, Vol. 204, p. 117918. ISSN 1359-4311.

Peixer, G., Lozano, J.A. and Barbosa, J.R., 2017. "Performance evaluation of AMRs using different casings". In *Book of Abstracts for the Danish Days on Caloric Materials and Devices*. Roskilde, Denmark.

Peixer, G.F., Dutra, S.L., Calomeno, R.S., Sá, N.M., Lang, G.B., Lozano, J.A. and Barbosa Jr., J.R., 2022. "Influence of heat exchanger design on the thermal performance of a domestic wine cooler driven by a magnetic refrigeration system". *Anais da Academia Brasileira de Ciências*, Vol. 94, No. 1. doi:10.1590/0001-3765202220200563.

Peixer, G.F., Nakashima, A.T., Lozano, J.A. and Barbosa, J.R., 2023a. "System-level multi-objective optimization of a magnetic air conditioner through coupling of artificial neural networks and genetic algorithms". *Applied Thermal Engineering*, Vol. 227, p. 120368. ISSN 1359-4311.

Peixer, G.F., Silva, M.C., Lorenzoni, A., Hoffmann, G., dos Santos, D., do Rosário, G.M., Pagnan, E., Teza, H.F., Silva, P.M., Dutra, S.L., Ribeiro, M.C., Rosa, M.A., Döring, A., Vieira, B.P., Nakashima, A.T., Wendhausen, P.A., Teixeira, C.S., Lozano, J.A. and Barbosa, J.R., 2023b. "A magnetocaloric air-conditioning system prototype". *International Journal of Refrigeration*. ISSN 0140-7007. doi:https://doi.org/10.1016/j.ijrefrig.2023.03.014.

Qian, S., Nasuta, D., Rhoads, A. and Wang, Y., 2016. "Not-in-kind cooling technologies: a quantitative comparison of refrigerants and system performance. technologies de refroidissement alternatives: une comparaison quantitative des frigorigènes et de la performance du système." *International Journal of Refrigeration*, Vol. 62, pp. 177–192. doi:10.1016/j.ijrefrig.2016.04.005.

Santos, D., Dutra, S., Ribeiro, M., Lorenzoni, A., Rosário, G., Silva, M., Hoffmann, G., Peixer, G., Lozano, J. and Barbosa Jr, J., 2021. "Designing a hydraulic management system for a large-scale magnetic refrigerator". In *9th IIR International Conference on Caloric Cooling and Applications of Caloric Materials, Maryland, June*. pp. 07–11.

Schwedersky, B.B., Flesch, R.C. and Rovea, S.B., 2022. "Echo state networks for online, multi-step mpc relevant identification". *Engineering Applications of Artificial Intelligence*, Vol. 108, p. 104596. ISSN 0952-1976.

Silva, M.C.R., Rosário, G.M., Dutra, S., Capovilla, M.S., Lima, R., Lorenzoni, A., Dos Santos, D., Hoffmann, G.,

Fidelis Peixer, G., Lozano, J. and Barbosa, J., 2021. "Development and characterization of a calibrated calorimeter to evaluate air conditioning systems". In *Proceedings of the 26th International Congress of Mechanical Engineering*. ABCM.

Vieira, B.P., Bez, H.N., Kuepferling, M., Rosa, M.A., Schafer, D., Plá Cid, C.C., Vieyra, H.A., Basso, V., Lozano, J.A. and Barbosa, J.R., 2020. "Magnetocaloric properties of spheroidal La(Fe,Mn,Si)13Hy granules and their performance in epoxy-bonded active magnetic regenerators". *Applied Thermal Engineering*, Vol. 183. ISSN 13594311.

Xiong, T., Bao, Y. and Hu, Z., 2013. "Beyond one-step-ahead forecasting: Evaluation of alternative multi-step-ahead forecasting models for crude oil prices". *Energy Economics*, Vol. 40, pp. 405–415. ISSN 0140-9883.

7. RESPONSIBILITY NOTICE

The author(s) is (are) solely responsible for the printed material included in this paper.